Open Journal of Physical Science (OJPS)
ISSN: 2734-2123
Article Details:
DOI: 10.52417/ojps.v5i1.626
Article Ref. No.: OJPS0501001-557
Volume: 5; Issue: 1, Pages: 01- 17 (2024)
Accepted Date: 28th May, 2024

CrossMark
click for updates

Open Journals Nigeria (OJN)
Open Access | Bi-annual | Peer-reviewed
www.openjournalsnigeria.org.ng
editorial@openjournalsnigeria.org.ng

RESEARCH ARTICLE OJPS0501001-557

METAMORPHISM AND DEFORMATION OF GOLD-BEARING NEOPROTEROZOIC WONAKA SCHIST BELT, NORTHWEST-NIGERIA.

Umar, U. S.

Department of Applied Geology, Abubakar Tafawa Balewa University, Bauchi

***Corresponding Author Email:** usumar@atbu.edu.ng*

ABSTRACT

The role of metamorphism and deformation is indispensable in the occurrences of gold mineralization worldwide. In this work, deformation and metamorphic conditions for gold-bearing Neoproterozoic Wonaka Schist Belt; located around Kutcheri town of Tsafe Local Government of Zamfara State, was investigated. This is achieved using metamorphic litho-minerals obtained from ternary plots via X-Ray fluorescence (XRF) geochemical data, and directly using minerals phases from X-Ray Diffraction (XRD) technique. Index minerals identified from petrographic analysis previously suggest low to medium-grade metamorphism (M1). XRD analysis indicates quartz, albite, oligoclase, microcline, chlorite, and biotite, suggesting greenschist to lower amphibolite facies (M2). Sillimanite, andalusite, kyanite, staurolite, chlorite, biotite, and garnet were identified from the ternary plots using XRF major oxides, indicating upper amphibolite to granulite facies metamorphism (M3). This is typical of prograde metamorphism, granulite facie metamorphic grade is indicated. Na_2O/Al_2O_3 versus K_2O/Al_2O_3 for petrogenetic character suggests shale provenance, while the trace elements spider diagram indicates Wonaka litho-units as co-genetic compositionally, as high concentrations of V and Cr linked the petrogenetic affinity to mafic sources. Three circles of deformations are indicated; ductile deformation (D1) of the paleosome Schist producing foliations and lineation, brittle type (D2) in mid Pan-African and was accompanied by several fractures and felsic intrusions. Late Pan-African (D3) involves the folding of banded orthogneisses, the development of boudinage as well as intense shearing (ductile fault). Geospatial analysis of the fractures suggests that they represent regional Pan-African sutures cross-cutting Nigeria into the Atlantic and up to South American plate. The research therefore concludes that Au-fluid emanating through this regional event, utilizes D2 as channel ways and loci. D3 with M3 engulfed the entire structures repositioning the geometry to its present disposition.

Keywords: *Deformation, Geochemistry, Gold Mineralization, Metamorphism, Wonaka Schist Belt.*

INTRODUCTION

Wonaka Schist Belt is one of the eleven Upper Proterozoic Schist Belts of the Nigerian sector of the Pan-African province of West Africa (Turner, 1983). It is located Northwest of the Karaukarau Belt which the duo believed to represent the cooling ages of the Pan-African episode (Harper *et al.,* 1973), K-Ar geochronology points to 515 to 550 Ma. The Belt is geographically located around Kutcheri town in Tsafe Local Government of Zamfara State. Metamorphism and Deformation usually go hand in hand, while the former defines chemical and mineralogical readjustment of preexisting rock, the latter denotes structural and textural changes a given rock has undergone due to mainly influence of stress over a geologic time. Depending on the agent or weights of agents inducing the metamorphism, most metamorphic rocks are also almost equally deformed and vice versa (Winter, 2001).

Wonaka Schist Belt is distinctive in metamorphism and mineralogy. Due to its close association with large granitic and granodioritic batholithic masses, Turner, (1983) believed it is a high-temperature low-pressure type. However, Umar *et al.,* (2022) indicate the Belt as typical of a prograde metamorphic condition. Muscovites identified during microstructural analysis point to greenschist facie while field litho-configurations suggest granulite facie. Wonaka rocks using both micro and macro structures were termed Wonaka Migmatites (Figure 1) and further grouped into types I, II, III, and IV for Banded Orthogneisses, Stromatic, Schlieren, and Nebulitic Migmatites respectively. This work aims to provide the history of deformation as well as metamorphic conditions of the gold-bearing Wonaka Schist Belt, these petrologic attributes would provide the needed understanding of the Belt's gold mineralization potentials and assist in exploration planning. It was achieved using field and geochemical data (major and trace elements) generated via X-ray fluorescence (XRF) as well as mineral phases via X-ray diffraction (XRD) technique.

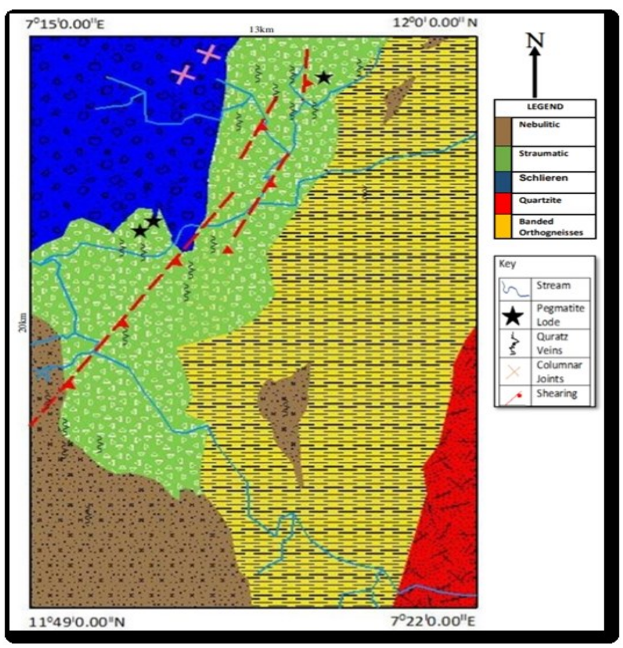

Figure 1: Litho-structural Map of the study area.

Source: Uma r *et al.,* (2022)

MTERIALS AND METHODS

Field work was conducted during which measurements and photographs of the structures were taken. 30 samples from different parts of this Schist Belt were collected, sorted, and analyzed for both petrographic study and geochemical analysis. Since one of the prime motives of the work is to understand the petrologic relationship between gold mineralization within the area and host lithologies, emphasis was given to quartzofeldspathic rocks during sample selection for the geochemical analysis.

Seven selected samples were sent to the Nigerian Geological Survey Agency (NGSA) geochemical laboratory Kaduna Nigeria, for whole-rock plus trace element analysis using the X-ray fluorescence (XRF) technique. XRF which is a non-destructive analytical technique was used to determine the elemental composition of the rock samples. XRF analyzers determined the chemistry of the samples by measuring the fluorescent (or secondary) X-ray emitted from a sample after it was excited by a primary X-ray source. Each of the elements present in the sample produced a set of characteristic fluorescent X-rays that are unique for that specific element (Chen, *et al.,* 2008). Accordingly, ten major elements and twenty trace elements were investigated from each of the seven samples analyzed.

Five (5) samples from the same source and location were analyzed using the X-ray diffraction technique (XRD) in the NGSA Laboratory Kaduna. Mineral phases including textural and crystallographic properties of the rock samples have been indicated. This has gone a long way to complement mineral identification conducted via a petrographic microscope. Identification of phases was achieved by comparison of the acquired data to that in reference databases. The XRD test method was performed by directing an X-ray beam at a sample and measuring the scattered intensity as a function of the outgoing direction. Once the beam is separated, the scatter, also called a diffraction pattern, indicates the sample's crystalline structure. The refinement technique is then used to characterize the crystal structure which is provided in the observed pattern.

RESULTS AND DISCUSSIONS

XRF GEOCHEMICAL RESULT

Results of the chemical analysis for both major and trace elements of selected samples representative of the Wonaka Schist Belt lithology are given in Tables 1 and 2 respectively. Concentrations of ten (10) major elements in oxide percentages (Table 1) and twenty (20) trace elements in parts per million (ppm) are presented (Table 2). These samples represent the varying lithologies encountered within the study area; samples L13 and L9 are the migmatites that flank the upgraded Wonaka biotite Schist, K19, K2, K26, and K12a are representative samples of the upgraded Wonaka biotite Schist while A2 is a quartzite coexisting alongside phyllites. Gold is primarily known and has been reported to occur within quartz/pegmatite bodies and stringers, this is consistent with earlier works (Akande and Fakorede, 1988; Akande, 1991; Garba, 2002; 2003). This justifies the high SiO_2 of samples K12a, A2, and L9 since they are quartz, quartzite, and pegmatite respectively. Some of the oxides were below the detection limit and were presented as ND (Not Detected), for example, SO_3 in K19, A2, and K12a, MgO in A2, K_2O in A2, and K12a. The oxides data also indicated that the upgraded Schist has poor K_2O and flanking nebulitic migmatites relatively fair (Table 1), the nebulitic migmatites are more potassic than banded orthogneisses.

The trace element data shows a high concentration of V and Cr and is consistence with earlier works (Kraemer and Rydell, 1972; Campo and Guevara, 2005), and indicates that metapelites are rich in such elements especially those that have a mafic affinity. The value of Cu has enhanced the possibility of Cu mineralization since the value is way beyond the known background of 42 ppm in ultramafic rocks and 72 ppm in mafic rocks which is the highest in all rock types.

Table 1: Major Oxides XRF Geochemical Data for Wonaka Schist Belt.

Oxides Composition (%)	**L 13 (Nebutic Migmatite)**	**K 19 (Biotite Schist)**	**K 2 (Biotite Schist)**	**A 2 (Quartzite)**	**L 9 (Pegma tite)**	**K 26 (Biotite Schist)**	**K 12a (Quartz)**
SiO_2	73	65	57.01	96.6	81.2	72.8	97
CaO	1.56	4.07	3.7	0.14	0.8	0.84	0.7
MgO	0.33	2	1.02	ND	0.09	0.32	0.02
SO_3	0.014	ND	0.48	ND	0.42	0.084	ND
K_2O	3.4	0.88	1.2	ND	4.6	1	ND
Na_2O	2	1.78	1.4	0.01	1.7	1.3	0.26
TiO_2	1.27	1.7	2.54	0.072	0.17	1.6	0.018
MnO	0.21	0.23	0.24	0.015	0.063	0.18	0.022
Fe_2O_3	4.16	10.2	13.3	1.87	1.78	7.12	0.7
Al_2O_3	13.01	12.46	13.04	0.36	5.4	12.46	0.46
LOI	1.01	1.42	6.46	0.62	1.06	1.41	0.42
Total	99.964	99.74	100.39	99.687	97.283	99.114	99.6

Table 2: Trace Element XRF Geochemical Data for Wonaka Schist Belt.

Elements (ppm)	L 13 (Nebutic Migmatite)	K 19 (Biotite Schist)	K 2 (Biotite Schist)	A 2 (Quartzite)	L 9 (Pegmatite)	K 26 (Biotite Schist)	K 12a (Quartz)
V	60.06	300.24	530	100	160.06	720	280
Cr	28.4	220.1	250.44	60.1	180.4	360.01	470.87
Cu	300	370.3	680	15	240	440.1	96.2
Sr	900.55	1870	2100	<0.01	<0.01	65.044	130
Zr	189.1	1300	100	<0.01	640	40	20.77
Zn	180	330.3	20.4	<0.01	120.34	360.2	14
Pb	200	570	100	160	250	10.21	10
Ba	2100	600	200	790	60	600	50
Ga	15.18	28.3	38.06	10.2	7.1	12.01	7.01
Ge	<0.01	<0.01	<0.01	<0.01	<0.01	2	0.51
As	7	<0.01	<0.01	<0.01	8.8	<0.01	0.8
Y	2.01	<0.01	3.13	<0.01	4.81	<0.01	<0.01
Ni	<0.01	<0.01	<0.01	<0.01	<0.01	<0.01	<0.01
Rb	189.3	157	186.7	<0.01	115	131.2	87.44
Nb	<0.01	<0.01	<0.01	<0.01	3.8	<0.01	<0.01
Ta	<0.01	<0.01	<0.01	<0.01	1.14	<0.01	<0.01
W	<0.01	<0.01	<0.01	<0.01	0.74	<0.01	<0.01
Hf	58.2	56.46	40.46	<0.01	36.24	43.1	5.44
Sb	<0.01	0.5	0.47	<0.01	<0.01	<0.01	0.03
Pr	<0.01	<0.01	<0.01	0.68	<0.01	<0.01	<0.01

ND = Not Detected

TERNARY PLOTS (ACF, AKF, AFM, AND AKFM)

The models and studies of these ternary plots in understanding metamorphic rocks, especially metamorphic mineral paragenesis were enhanced by Helmut and Winkler, (1974). This was done to define metamorphic minerals and use them as index minerals to predict their condition of formation which ultimately gives the metamorphic grade. The ACF (A: Al_2O_3, C: CaO, and F: FeO + MgO) diagram was plotted using the chemical analysis of the Wonaka samples (major elements). At first, the concentrations were recalculated to molecular proportions by dividing the molecular weight of each oxide constituent by the molecular weight of that oxide. A wide variety of rock compositions were grouped as pelitic, quartzo-feldspathic, basic, and calcareous and the fields are shown in Figure 2. Most shales plot in the field of pelitic rocks, quartzo-feldspathic rocks like feldspathic sandstones, granites, and rhyolites will plot in the Quartzo-Feldspathic field.

The ACF diagram indicate that the Wonaka Schist Belt are within the boundaries of pelitic sediments which means the Schist Belt was a result of metamorphism of fine-grained sedimentary rocks as in Winter, (2001). The diagram shows the plotting positions of some of the more common minerals that occur in metamorphic rocks. These mineral paragenesis would be assessed to understand the degree of metamorphism, depth as well as temperature and pressure conditions under which they occur.

In AKF diagrams (A = [Al_2O_3 + Fe_2O_3] - [Na_2O + K_2O + CaO], K = [K_2O], F= [FeO + MgO + MnO]) it is assumed that both alkali feldspar and plagioclase feldspar can be present, thus the amount of Al_2O_3 that is used is the excess Al_2O_3 after providing the feldspars. Minerals are plotted in the same way as was done for the ACF diagrams. The AKF diagram for the Wonaka study area showing the plotting positions of common metamorphic minerals is shown in Figure 2. AKF diagrams are used for CaO-deficient, K_2O-rich rocks, whereas ACF diagrams are for both Al_2O_3 and CaO-rich rocks.

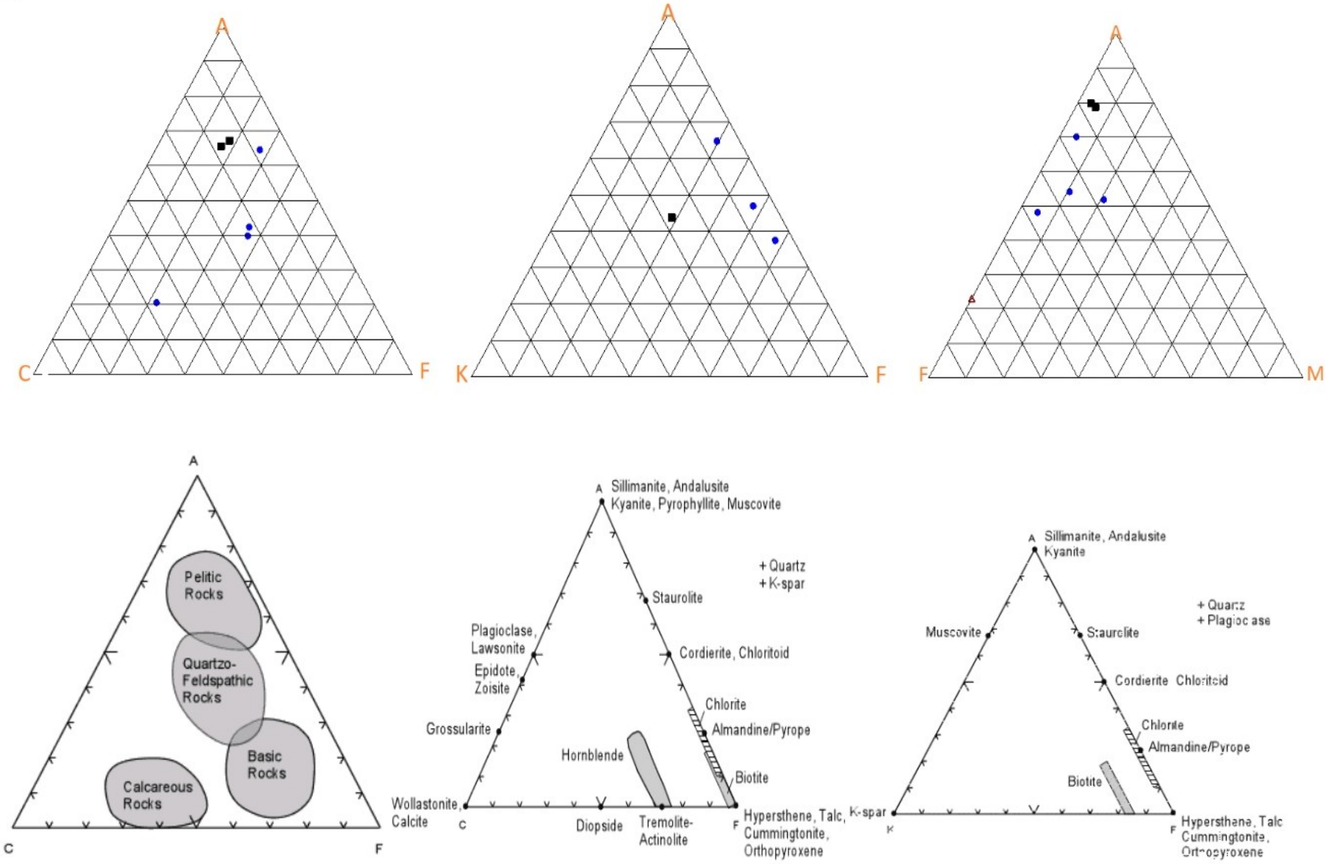

Figure 2: ACF, AKF, and AFM Ternary plots for Wonaka Metapelites Showing Metamorphic Minerals.

AKFM PROJECTION ONTO AFM

The ACF and AKF diagrams are fairly simple and very useful. One of the problems associated with ACF and AKF diagrams is that Fe and Mg are assumed to substitute for one another and act as a single component, Fe-rich olivine is fayalite and Mg-rich olivine is forsterite. However, in natural minerals, the composition of Fe - Mg solid solution is dependent on temperature and pressure. Thus, in treating Fe and Mg as a single component, some information is lost. Helmut and Winkler (1974) developed a projected diagram that considers possible variations in the Mg/(Mg+Fe) ratios in ferromagnesium minerals and has proven very useful in understanding metamorphosed pelitic sediments. In this case, it starts with the 5-component system SiO_2 - Al_2O_3 - K_2O - FeO - MgO and ignores minor components in pelitic rocks like CaO and Na_2O. Because quartz is a ubiquitous phase in metamorphosed pelitic rocks, the five-component system is projected onto the four-component system Al_2O_3 - K_2O - FeO-MgO as shown in Figure 3, since muscovite is a common mineral in these rocks, all compositions are projected from muscovite onto the front face of the diagram, (Al_2O_3 - FeO - MgO). So that the front face of the diagram becomes the AFM diagram. Minerals that contain no K_2O like andalusite, kyanite, and sillimanite plot at the 'A' corner of the diagram, and minerals like staurolite, chloritoid (Ctd), chlorite, and garnet plot on the front face of the diagram. Biotite, however, does contain K_2O and has varying amounts of Al_2O_3 and thus is a solid solution that lies in the four-component system. Because muscovite is relatively K-poor, this results in biotite being projected to negative values of Al_2O_3. For the AFM, A = [Al_2O_3 - 3 K_2O], F = [FeO], M = [MgO].

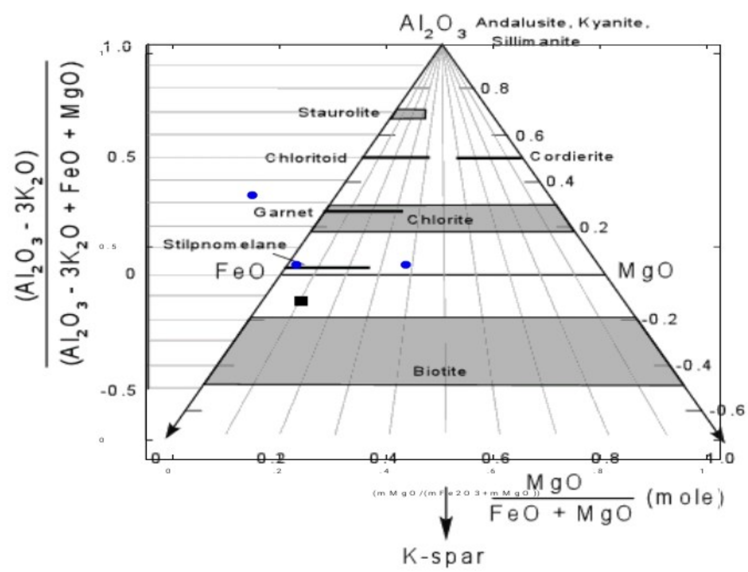

Figure 3: Projection of the AKFM Plot Onto the AFM Model.

Using these parameters, one can grid off the AFM diagram with the vertical scale represented by the normalized values for the A parameter - [Al_2O_3 - 3 K_2O] / [Al_2O_3 - 3 K_2O + FeO + MgO] and the horizontal position based on the ratio of MgO / (FeO + Mg) as seen in Figure 3. These values are obtained after converting the chemical analysis of the rock to molecular proportions. The projection from muscovite works well for metamorphic rocks that contain muscovite. Muscovite appears to be the dominant mineral even during the petrographic analysis of these samples, it is however known that at higher grades of metamorphism, in the upper amphibolite facies and the granulite facies, muscovite becomes unstable and is replaced by K-feldspar + quartz + Al_2SiO_5.

THE PETROGENETIC CHARACTER

The petrogenetic character of the mica Schist as indicated on the Na_2O/Al_2O_3 against K_2O/Al_2O_3 diagram after Garrels and Mackenzie (1971) shows the biotite Schist to be of sedimentary origin (Figure 4), and thus has a sedimentary protolith. Sedimentary petrologists have shown that virtually all shales have lower Na_2O/Al_2O_3 values than the lowest limits of the ratio found in igneous rocks, whether mafic or felsic as thus indicated in the plot.

The trace elements spider diagram in Figure 5 was plotted for comparison with that of the average continental crust of Weaver and Tarney (1984), given the fact that the continental crust has been extracted from the mantle, its composition is, therefore, an indispensable key in understanding the chemical evolution of the earth. Attempting to model its average chemical composition is difficult because of its complexity and heterogeneity. Thus, estimates of Weaver and Tarney (1984), as well as Gao *et al*. (1998) and Shaw *et al.* (2011) are adopted. The trace elements spider as can be seen in Figure 5 displays varying compositions as represented by the respective points. However, it indicates that the rocks are co-genetic, suggesting compositional contamination during circles of remobilisation at stages of metamorphism and alterations.

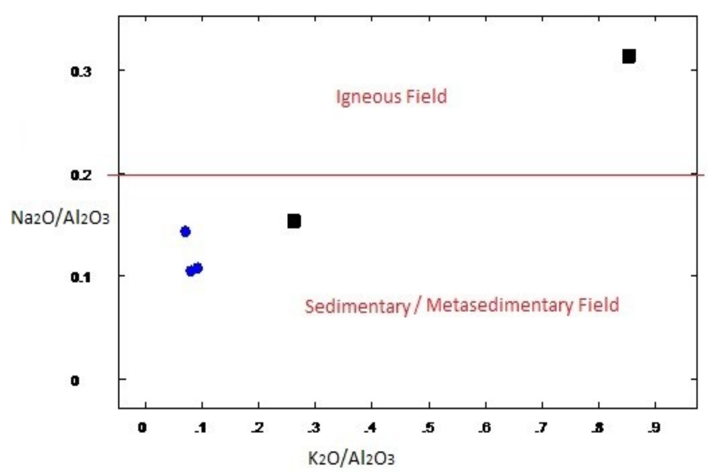

Figure 4: Na_2O/Al_2O_3 Versus K_2O/Al_2O_3 Petrogenetic Characterization indicating Sedimentary Origin.

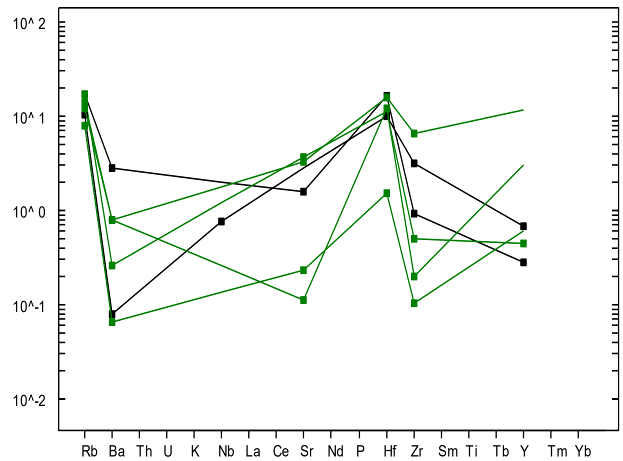

Figure 5: Spider Diagram for Wonaka Schist Indicating Alliance with Average Continental Crust.

THE XRD RESULTS

The XRD results for the selected samples are presented in Figure 6 (A to D) for samples A2, K12a, K26, and L9 respectively. Sample A2 and K12a are respectively quartzite and pegmatites. The chemical data for these samples is in Table 1. The quartzite occurred in association with the phyllites, which are muscovite-rich. The pegmatite was collected from within the upgraded biotite Schist of the Wonaka Schist Belt. Mineral phases identified are quartz and albite (Na-riched plagioclase feldspar). This is expected given the mineralogy of pegmatite as a quartz-feldspar dominant igneous rock.

Sample K26 is dominated by quartz, biotite, oligoclase, and chlorite, representing the upgraded biotite Schist. Sample L9 comes from the flanking nebulitic migmatites, and it is mineralogically dominated by quartz, albite, microcline, and biotite. The chemical data for these samples is presented in Table 1. The XRD is of special importance since it picks and defines mineral phases that constitute the rock, because minerals like oligoclase, albite, and others forming solid solutions of the plagioclase, could not be identified with certainty through petrography. Minerals identified are used as index minerals to interpret metamorphic conditions since they have formed the mineral configurations for the particular metamorphic mineral assemblages. Textural characteristics of these rocks have been deduced from the XRD results because the degree of proximities within the peaks explains how fine or coarse the rock sample was. More congested peaks denote more finer samples and vice-versa. See Figure 6 (A and B) for sample A2 and sample K12a in comparison to Figure 15 (C and D) for samples K26 and L9.

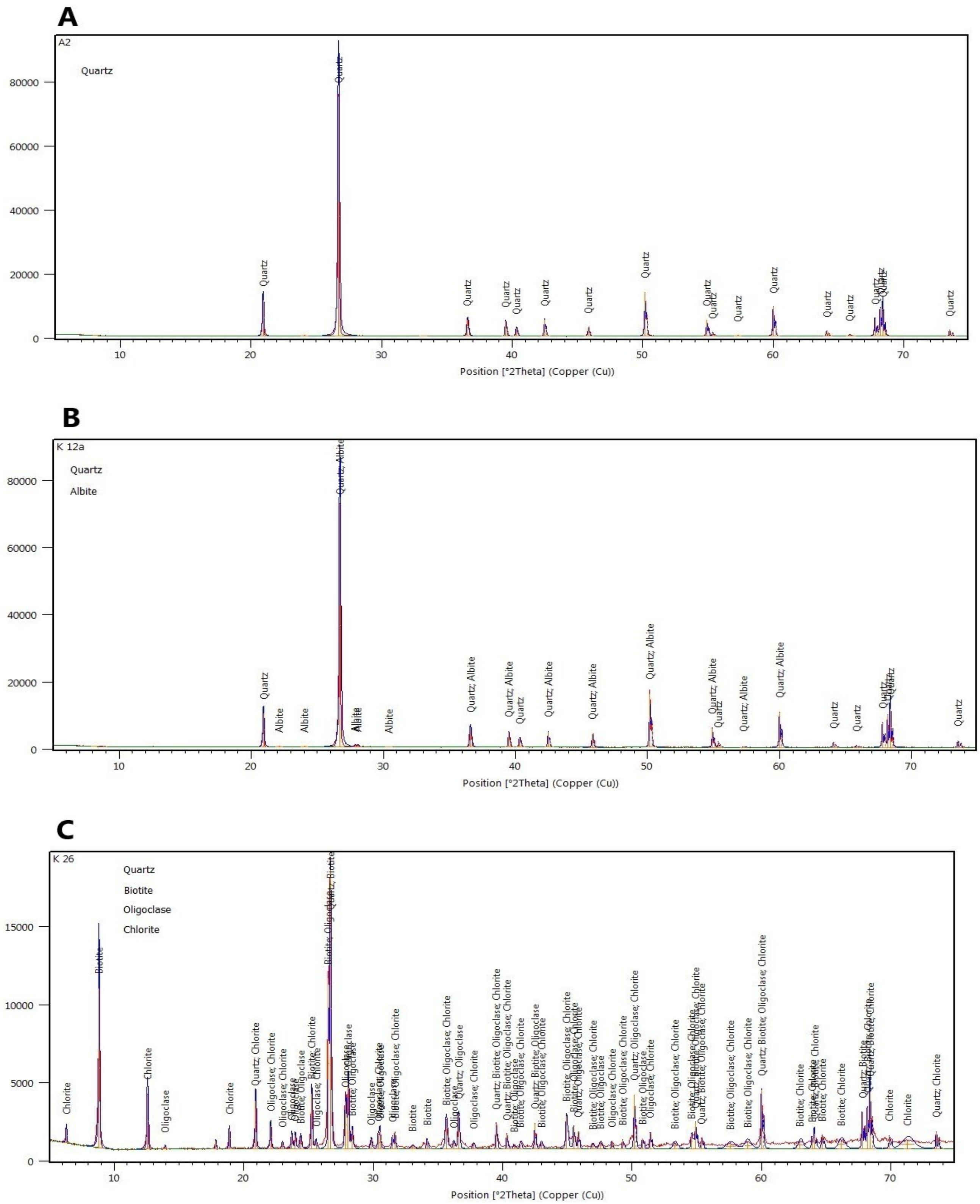
A
A2
Quartz
80000
60000
40000
20000
0
10
20
30
40
50
60
70
Position [°2Theta] (Copper (Cu))
B
K 12a
Quartz
Albite
80000
60000
40000
20000
0
10
20
30
40
50
60
70
Position [°2Theta] (Copper (Cu))
C
K 26
Quartz
Biotite
Oligoclase
Chlorite
15000
10000
5000
0
10
20
30
40
50
60
70
Position [°2Theta] (Copper (Cu))

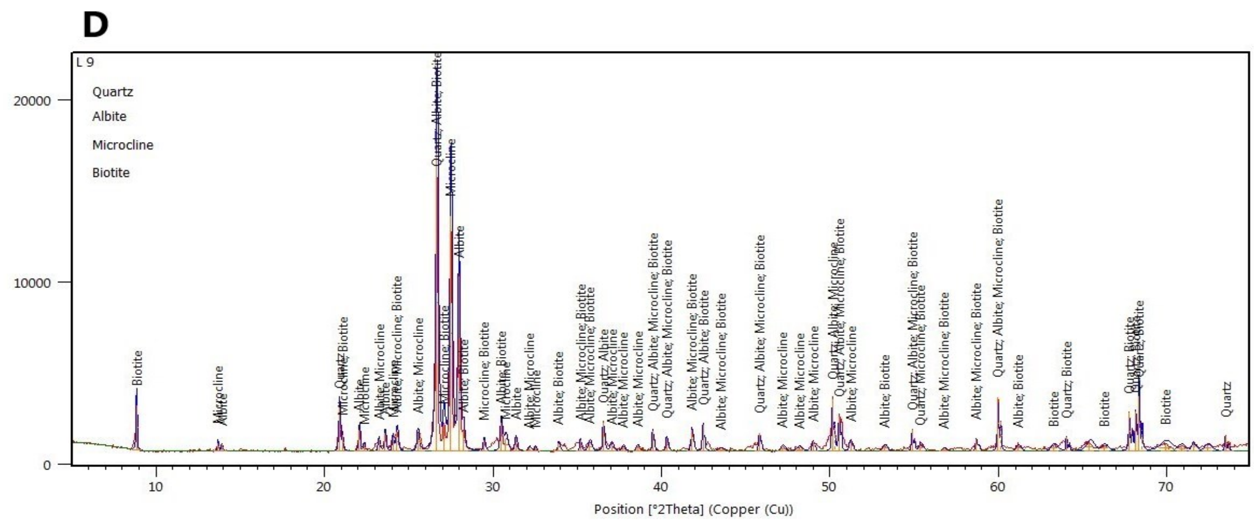

Figure 6: Presentation of XRD Results for Sample A2, K12a, K26, and L9 Respectively, showing the Mineral Phases.

GRADE OF METAMORPHISM FOR WONAKA SCHIST BELT

Table 4 is the summary of metamorphic index minerals generated from the three methods; (1) petrography (Umar *et al.,* 2022), (2) Ternary plots of AFM using major elements XRF chemical analysis, and (3) the XRD mineral analysis. Minerals identified via each of these methods are mentioned and their corresponding metamorphic grade is indicated. The general facie type, protolith for each group of mineral assemblages representing different metamorphic conditions are presented in Table 4. The ternary plots: ACF, AKF, and AFM are important in defining metamorphic mineral assemblages, as this would enable the identification of minerals that were not detected during either petrography or XRD analysis. The ACF diagram in Figure 2 indicated that the rocks were metamorphosed pelitic sediments and felspathic rocks. This confirms findings from the fieldwork since quartzite is among the lithologies of the Wanaka Schist Belt. This is assisting with the controversy in the protolith for the Schist Belt.

The constituent minerals according to the XRD (Figure 6) include quartz, albite, oligoclase, chlorite, biotite, and microcline. Muscovite was the common and most abundant mineral in all the analysed samples under microstructural analysis (Umar *et al.,* 2022), while metamorphic minerals established as common through ACF, AKF, and AFM are sillimanite, andalusite, kyanite, staurolite, chlorite, biotite, and garnet. Quartz + muscovite and or plagioclase are seen to be constant for all the studied samples as plotted in ACF, AKF as well as AFM diagrams (Figures 2 and 3). This type of metamorphic mineral configuration is similar to that ranging from amphibolite to granulite facies metamorphism of Table 4. The Table equally indicated that the protolith for the Wonaka Schist Belt is pelitic rock (fine-grain sedimentary rock). This study therefore indicates evidence of amphibolite to granulite facies metamorphism. However, authors (Turner, 1983; Danbatta, 1999; Garba, 2002; Ramadan *et al.,* 2011) believed that Schist Belts in Nigeria are low to medium-grade metasediments and metavolcanic that were intruded by Pan-African granitoids. The range of temperature, pressure, and depth at which this condition of metamorphism occurs is therefore generated in Table 3 as 600-900 ^{o}C, 6-8 Kbars, and in a depth of about 15-30 km respectively.

Table 3: Facie, Protolith and Mineral Assemblage for Different Metamorphic Conditions

Facies	Pelitic
Zeolite 100-200 ^{0}C	Interlayered Smectite/Chlorite Calcite
Prehnite Pumpellyte 150-300 ^{0}C	Prehnite Pumpellyte, Calcite, Chlorite, Albite
Greenschist 300-450 ^{0}C	Muscovite, Chlorite, Quartz, Albite, Biotite, Garnet
Epidote Amphibolite 450-550 ^{0}C	Muscovite, Biotite, Garnet, Albite, Quzrtz
Amphibolite 500-700 ^{0}C	Garnet, Biotite,Muscovite, Quartz, Staurolite, Kyanite or Sillimanite
Granulite 700-900 ^{0}C	Garnet, Kspar, Sillimanite or Kyanite, Quartz, Plagioclase, Hypersthene

Ghent (2020)

HISTORY OF METAMORPHISM AND DEFORMATION

Exposures of the Schist shown in Figure 7, which represent supra crustal cover (Danbatta and Garba, 2007) have shown evidence of polycyclic metamorphism and deformations (Table 4) and in consistence with earlier works of Ajibade and Woakes, (1988); McCurry, (1988). After deposition and diagenesis of the pelitic sediments, the first transformation began with the coalescence of the quartz and feldspar crystals forming platy transparent minerals of the muscovite family. Muscovite is used as a geobarometer to indicate the degree of metamorphism under prograde conditions (Winter, 2001). This indicates Wonaka Schist as low to medium-grade metamorphic rocks (M1) and it is in consistence with the work of Turner, (1983); and Garba, (2000; 2002). As metamorphism progresses, biotite enters the mineral set, the fissility of the shales hardens and foliations of the phyllites become more prominent and stronger. This is the historicity of the Schist in medium-grade metamorphism (Winter, 2001; Mukherjee, 2011). The Schistocity of the Schist is the preserved but remodified laminations of the pelitic sedimentary rock before low to medium-grade metamorphism. This stage was accompanied by higher-grade metamorphism into amphibolite facie probably during mid Pan-African (M2) Table 4.

The last metamorphic event was the migmatisation of the entire lithological unit which is granulite facie metamorphism (M3). This is evident by the injection of felsic melt, though probably less than 30 % by volume (Sawyer, 2014), into existing fractures thereby raising the temperature to the point of partial melting and segregating the darker minerals referred to as the residuum to form bands of leucosome and melanosomes. According to Vigneresse and Bury (2000), an irregularly developed network of deformed leucosome and melanosome bands is typical of migmatisation. This took place during the late Pan-African (Ukaegbu and Oti, 2005). This phase is accompanied by regional ductile deformation during the compressive episode of the Pan-African closure. In this case, the banded orthogneisses were folded along with the felsic leucosome (Figure 7), indicating this phase of ductile deformation postdating the migmatisation.

Table 4: Summary of Metamorphism and Deformation for Wonaka Schist Belt.

Method	Metamorphic Minerals	Metamorphic Grade	Deformation
Petrography	Quartz, Muscovite, Albite, Microcline, Biotite and Opaque Minerals	Low to medium-grade metamorphism (M1)	Ductile deformation of the paleo some Schist producing foliations and lineation (D1)
XRD	Quartz, Albite, Oligoclase, Microcline, Chlorite and Biotite	Greenschist to lower amphibolite metamorphism (M2)	Brittle deformation producing fractures, faults and joints (D2)
Ternary plots	Sillimanite, Andalusite, Kyanite, Straurolite, Chlorite, Biotite and Garnet, While Quartz + Muscovite Are Constant	Upper amphibolite to granulite facie metamorphism (M3)	Plastic deformation and migmatisation producing shear zones, boudins and ptygmatic folding (D3)

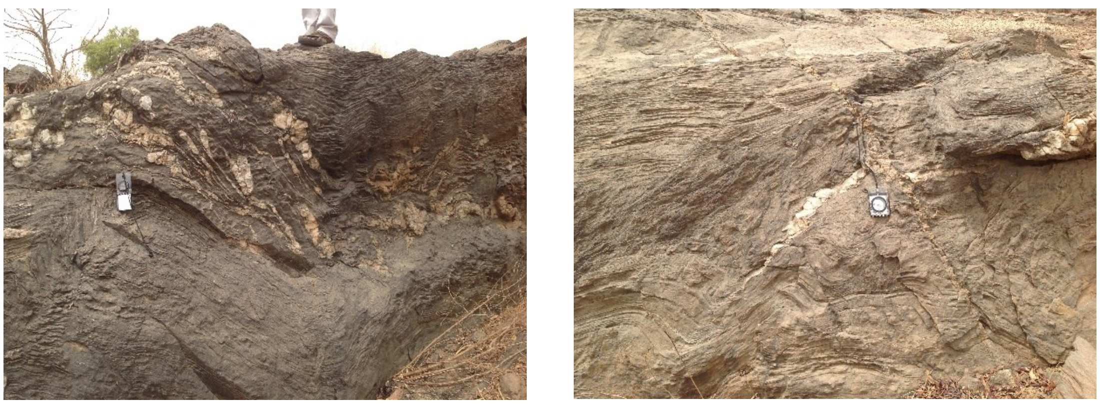

Figure 7: Coexistence of leucosome and melanosome in Wonaka Schist Belt, indicating a degree of metamorphism and amount of deformation.

Apart from intense metamorphism, the Wonaka Schist Belt has undergone at least three circles of deformation (Table 4). The first is a ductile deformation (D1) of the paleosome Schist producing foliations and lineation. It is intricately related and dependent on the metamorphic event transforming the pelitic sediments into Schist. The second set of deformation (D2) was a brittle type, probably mid-Pan-African, and was accompanied by several fractures and felsic intrusions in the form of veins, dykes, and sills. The discordant intrusions mostly trend NW-SE. Local shear also developed, it was not clear whether it was linked to any regional event. During the third phase of deformation (D3) which may be late Pan-African, both host rocks and felsic intrusions were deformed in a manner that appears more plastic than brittle; folding of banded orthogneisses and the interconnected veins, development of boudinage structures as well intense shearing (ductile fault). This set of felsic intrusions trends mostly NE-SW conforming to regional Pan-African orogenic deformations.

Local shear zones which are precursors of the regional shear, trend NE-SW, and the limbs of the folds were mostly NW-SE, these conform to the general trend of Pan-African deformations. Structurally, shear zones are indispensable structures in the occurrence of world-class gold mineralisation, (Eisenlohr *et al.,* 1989; Castroviejo, 1990; Couture and Pilote, 1993).

Fractures within the study area especially those developed on schlieren migmatites were intense and mostly trended NE-SW, perpendicular to planes of gneissic foliations which were NW-SE. The geometry of these fractures is among the reasons to adjudge them as conjugate fracture systems that emanated from the regional transcurrent fault line (Figure 8) passing through the western half of Nigeria into the Atlantic and up to Brazil (South American plate). The water seen gushing from these planes suggests that the fractures serve as conduits to transmit this water from the fractured basement to the surface, while the foliation slaps redirect and channel it in the dendritic stream channels. This is an important mechanism of placer gold occurrence within the study area. This regional fault as indicated in Figure 8, passes through Nigeria into the Atlantic extending up to the South American plate. It is believed to have been formed during Neoproterozoic orogeny; these continents were once part of a supercontinent. Neoproterozoic orogeny was global; it is called Pan-African in Africa, Brasiliono in South America, Cadominan in Europe, and Bakilain in Asia. Most world-class gold deposits were found to possess a similar geospatial relationship with this fault as it cut across various continents.

Figure 8: Indication of the Regional Fault System Extending from Nigeria into the Atlantic and up to South America (Modified from Google Earth)

CONCLUSION

Analysis of the ternary plots using XRF chemical data as well as XRD mineral analysis indicates Wonaka Schist as a prograde metamorphic type with mineralogical evidence of low to medium-grade (M1), lower amphibolite (M2) and dominated by upper amphibolite to granulite facies metamorphic condition (M3). This is indicated to occur at a temperature range between 600 – 900 ^{0}C, a pressure of about 6 – 8 kb, and a depth of about 15 – 30 km. Field relations indicate typical migmatite terrain characterized by irregularly developed deformed felsic leucosome (neosome) and melanosomes (residuum).

Analysis of the petrogenetic character suggests that pelitic sediments and mafic volcanic rocks were believed to be deposited on the ocean flow at the oceanic basin setting during the early extensive stage of Pan-African orogeny. Findings indicated the pelitic sediments as shales and the mafic rocks to be pillow basalts. During the active stage of the orogeny, these materials were metamorphosed at the greenschist facie level and deformed (D_1) producing foliations and mineral lineation giving the Schistosity of the Schist. This is brought about by the pressure gradient resulting from the overburden weight of piling sediments.

The formation of the regional Pan-African transform fault and the intrusion of Pan-African granitoids during the Mesoproterozoic causes extensive brittle deformation of the metapelites and the metavolcanics, producing localised irregular fractures and faults (D_2), and set another cycle of metamorphism into amphibolite facies. The late Pan-African Neoproterozoic was compressive and characterised by crustal thickening of the Early Proterozoic supracrustal rocks. This causes partial melting at the deeper crust, generating the magmatic source hydrothermal fluid that utilises D_2 structures as both channel ways and as depository loci. However, Au deposition was successful for the interaction of this fluid with that produced via metamorphic dewatering of the shales. This provides the reduced condition for Au's precipitation. Migmatisation was intense, generated melt recrystallized into the (D_2) structures forming network of irregular leucosome as quartz/pegmatite veins, both neosome and paleosome have undergone plastic deformation during the compressive and final stage of the Pan-African producing folds, local boudinage, and shear zones (D_3).

REFERENCES

Ajibade, A.C. and Woakes, M. (1988). Proterozoic Crustal Development in the Pan-African Regime of Nigeria. *C. A. Kogbe Geology of Nigeria* **2**: 57-63.

Akande, S. O. (1991). Geological and Evolution of Gold Bearing Quartz Veins in the Nigerian Schist Belt. *Proceedings of the Symposium Brazil Gold* **90**(619): 195-198.

Akande, S. O. and Fakorede, O. (1988). Gold Mineralization in the Nigerian Schist Belt Becentennial *Gold 88, Melbourne* **1**: 139-141.

Campo, M. D. and Guevara, S. R. (2005). Provenance analysis and Tectonic Setting of the Late Neoproterozoic Metasedimentary Succession in NW Argentina. *Journal of South American Earth Science* **30**: 143-153. https://doi.:10.1016/j.jsames.2005.01.003

Castroviejo, R. (1990). Gold ores related to shear zones, West Santa Comba-Fervenza Area (Galicia, NW Spain): A mineralogical Study. *Mineral Deposita Springer-Verlag* **25**: 91-105.

Chen, Z. W., Gibson, W. M., and Huang, H. (2008). High Definition X-Ray Fluorescence: *Principles and Techmiques. Hindawi Publishing Coporation, X-Ray Optics and Instrumentation.* Volume 2008, Pp 1-10; doi:10.115/2008/318171

Couture, J. F. and Pilote, P. (1993). The Geology and Alteration Patterns of a Disseminated Shear Hosted Mesothermal Gold Deposit. *Economic Geology* **88**: 1664-1684.

Danbatta, U. A. (1999). The Geotectonic Evolution of the Kazaure Schist Belt in the Precambrian Basement of NW Nigeria. (Doctoral dissertation, Ahmadu Bello University Zaria 1999). *Academia.com*

Danbatta, U. A. and Garba, M. L. (2007). Geochemistry and Petrogenesis of Precambrian amphibolites in the Zurru Schist Belt, NW Nigeria. *Journal of Mining and Geology* **43**(1): 23-30.

Eisenlohr, D., Groves, D. L. and Partington, G. A. (1989). Craton Scale Shear Zones and their Significance to Archean Gold Mineralization in Western Australia. Mineral Deposita **24**: 182-235.

Gao, S., Zhang, B.R., Jin, Z. M., Kern, H., Luo, T. C. and Zhao, Z. D. (1998). How Mafic is the Lower Continental Crust? *Earth and Planet Science. Lett* **106**: 101–117.

Garba, I. (1992). Geology, Geochemistry and Origin of Gold Mineralization at Bin Yauri, Nigeria. Unpublished MSc Thesis Ahmadu Bello University, Zaria Nigeria. pp 1-126.

Garba, I. (2000). Gold Prospects of the Nigeria Pan African Terrain of West Africa. *Journal of Mining and Geology.* **36**(2): 123 – 135.

Garba, I. (2002). Late Pan-African Tectonics and Origin of Gold Mineralization and Rare-Metal Pegmatites in the Kushaka Schist Belt, Northwestern Nigeria. *Nigerian Journal of Mining and Geology*. **38**: 1-12.

Garrels, R.M. and Mackenzie, F.T. (1971). Evolution of Metasedimentary Rocks. *Norton and Company*, New York. 150-160.

Ghent, E. (2020). Metaorphic Fcaies: A Review and Some Suggestions for Changes. *The Canadian Mineralogist*; 58 (4), https://doi.org/10.3749/canmin.1900078

Helmut G. and Winkler, F. (1974). Classification Principles: Metamorphic Facies versus Metamorphic Grade. *Petrogenesis of Metamorphic Rocks* **2**: 54-62. https://link.springer.com

McCurry. P. (1988). A General Review of the Geology of the Precambrian to lower Paleozoic Rocks of Northern Nigeria. *C. A. Kogbe Geology of Nigeria* **2**(2): 13-23.

Mukherjee, S. (2011). Origin of Minerals and their Transformations in Nature Under Various Environmental Conditions in Applied Mineralogy. *Springer Dordrecht* **2**: 111-130. https://doi.org/10.1007/978-94-007-1162-4_9

Ramadan, T. M., Mohammed F. and Fatah A. (2011). Characterization of Gold Mineralization in Garin Hawal area, Kebbi State, *The Egyptian Journal of Remote Sensing and Space Sciences* **13**: 153-163.

Sawyer, E. W., (2014). The inception and growth of leucosome: microstructure at the start of melt segregation in migmatites. *Journal of Metamorphic Geology* **32**(7) 695-712, https://doi.org/10.1111/jmg.12088

Shaw, D. M., Dickin, A. P., Li, H. and Truscott, M. G. (2011). Crustal Geochemistry in the Wawa–Foleyet region, Ontario, Canadian. *Journal of Earth Sciences* **31**(7): 94-099.

Turner, D. C. (1983). Upper Proterozoic Schist in the Nigerian Sector of the Pan-African Province of West Africa. *C. A. Kogbe Geology of Nigeria*. **2**: 93-121.

Ukaegbu, V. and Oti, M. N. (2005). Structural Elements of the Pan-African Orogeny and their Geodynamic Implications in Obudu Plateau, Southeastern Nigeria. *Journal of Mining and Geology* **41**(1): 182-196. DOI: 10.4314/jmg.v41i1.18828

Umar, U.S., Haruna, A.I., Maigari, A.S., Muhammed, M., Yaro, U.Y., Yusuf, A.,Isah, A., Said, F. (2022). Litho-Structural Variations and Gold Mineralization of Neoproterozoic Wonaka Schist Belt: Field and Petrographic Approach. *Conference proceedings Nigerian Mining and Geosciences Society* 98-105.

Vigneresse, J. L. and Bury, J. P. (2000). Continues vs Discontinues Melt Segregation in Migmatites; *Tera Nove* **12**(4): 188-192.

Weaver, B.L. and Tarney, J. (1984). Major and Trace Element Composition of the Continental Lithosphere. *Physics and Chemistry of the Earth.* **15**: 39-68.

Winter, J. D. (2001). *An introduction to Igneous and Metamorphic Petrology*. Prentice Hall Upper Saddle River, New Jersey; Pp 526-585, ISBN 0-13-240342-0 1.